Cell Reports

T Cell Migration from Inflamed Skin to Draining Lymph Nodes Requires Intralymphatic Crawling Supported by ICAM-1/LFA-1 Interactions

Graphical Abstract

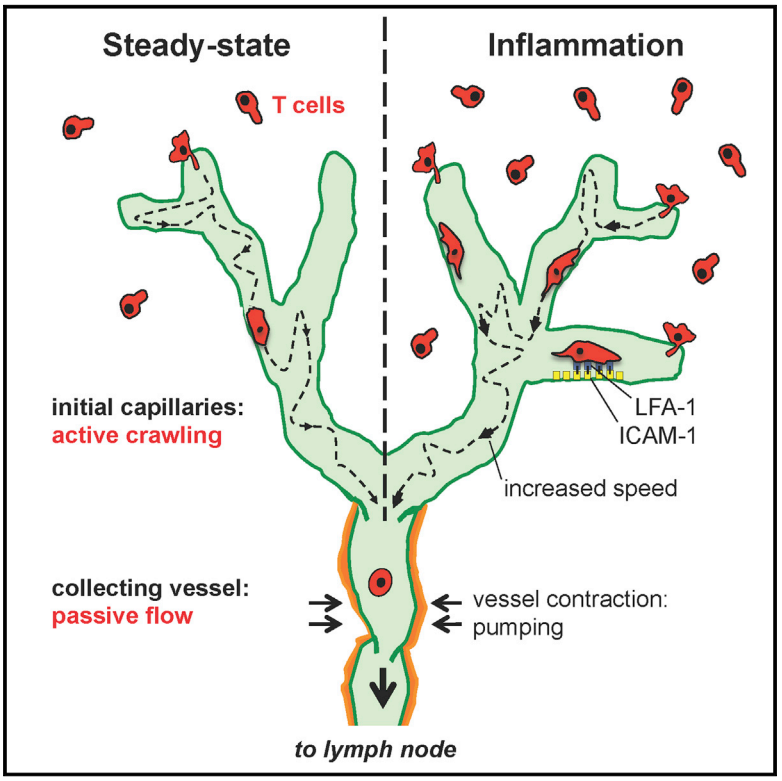

Authors

Alvaro Teijeira, Morgan C. Hunter, Erica Russo, ..., Michael Detmar, Ana Rouzaut, Cornelia Halin

Correspondence

cornelia.halin@pharma.ethz.ch

In Brief

T cell migration through afferent lymphatic vessels contributes to immune surveillance, but the cellular mechanisms of this process are largely unknown. Using intravital microscopy, Teijeira et al. show that T cells crawl in an ICAM-1/LFA-1-dependent manner within inflamed dermal lymphatic capillaries but only flow with lymph once in contracting collectors.

Highlights

- T cells crawl within initial lymphatic capillaries and flow in collecting vessels
- Tissue inflammation increases T cell speed within lymphatic capillaries
- Increased speed of T cells within lymphatic capillaries is ICAM-1/LFA-1 dependent
- ICAM-1/LFA-1 blockade reduces inflammatory T cell migration to draining lymph nodes

Teijeira et al., 2017, Cell Reports *18*, 857–865
January 24, 2017
http://dx.doi.org/10.1016/j.celrep.2016.12.078

Cell Reports
Report

T Cell Migration from Inflamed Skin to Draining Lymph Nodes Requires Intralymphatic Crawling Supported by ICAM-1/LFA-1 Interactions

Alvaro Teijeira,[1,2,6] Morgan C. Hunter,[1,6] Erica Russo,[1] Steven T. Proulx,[1] Thomas Frei,[1] Gudrun F. Debes,[3,4] Marc Coles,[5] Ignacio Melero,[2] Michael Detmar,[1] Ana Rouzaut,[2] and Cornelia Halin[1,7,*]
[1]Institute of Pharmaceutical Sciences, ETH Zurich, 8093 Zurich, Switzerland
[2]Department of Immunology and Immunotherapy, Center for Applied Medical Research, 31009 Pamplona, Spain
[3]School of Veterinary Medicine, University of Pennsylvania, Philadelphia, PA 19104, USA
[4]Department of Microbiology and Immunology, Thomas Jefferson University, Philadelphia, PA 19107, USA
[5]University of York, YO10 5DD York, UK
[6]Co-first author
[7]Lead Contact
*Correspondence: cornelia.halin@pharma.ethz.ch
http://dx.doi.org/10.1016/j.celrep.2016.12.078

SUMMARY

T cells are the most abundant cell type found in afferent lymph, but their migration through lymphatic vessels (LVs) remains poorly understood. Performing intravital microscopy in the murine skin, we imaged T cell migration through afferent LVs in vivo. T cells entered into and actively migrated within lymphatic capillaries but were passively transported in contractile collecting vessels. Intralymphatic T cell number and motility were increased during contact-hypersensitivity-induced inflammation and dependent on ICAM-1/LFA-1 interactions. In vitro, blockade of endothelial cell-expressed ICAM-1 reduced T cell adhesion, crawling, and transmigration across lymphatic endothelium and decreased T cell advancement from capillaries into lymphatic collectors in skin explants. In vivo, T cell migration to draining lymph nodes was significantly reduced upon ICAM-1 or LFA-1 blockade. Our findings indicate that T cell migration through LVs occurs in distinct steps and reveal a key role for ICAM-1/LFA-1 interactions in this process.

INTRODUCTION

Afferent lymphatic vessels (LVs) fulfill important immune functions by transporting soluble antigen and leukocytes such as dendritic cells (DCs) or recirculating T cells to draining lymph nodes (dLNs). T cells represent the major leukocyte cell type found in steady-state afferent lymph (Mackay et al., 1990; Young, 1999), and their migration through peripheral tissues and into afferent LVs is thought to contribute to immune surveillance. Most T cells found in afferent lymph of sheep and humans display a memory phenotype, with $CD4^+$ T cells outnumbering $CD8^+$ T cells by ~4- to 5-fold (Mackay et al., 1990; Yawalkar et al., 2000). The factors that determine T cell residence as compared to tissue egress into afferent LVs are not completely clear, but various studies have demonstrated that the CCR7/CCL21 pathway (Bromley et al., 2013; Debes et al., 2005) and sphingosine-1-phosphate (S1P) (Brown et al., 2010; Ledgerwood et al., 2008) play a pivotal role in this process. Recently, the phenotype of recirculating memory $CD4^+$ T cells (T_{RCM}) was described as $CCR7^{int/+}CD62L^{int}CD69^-CD103^{+/-}CCR4^{+/-}$E-selectin ligand$^+$. T_{RCM} were shown to migrate from skin to dLNs and from there back into circulation and to sites of cutaneous inflammation (Bromley et al., 2013).

Intravital microscopy (IVM) has recently shed light on the motility of individual T cells in peripheral tissues like the skin. In particular, IVM studies have revealed that under inflammatory conditions, both $CD4^+$ and $CD8^+$ effector T cells actively migrate in the dermis (Egawa et al., 2011). Conversely, in the memory phase following an antiviral immune response, $CD8^+$ cells were shown to remain arrested in the epidermis, whereas $CD4^+$ memory cells avidly migrated through the dermis (Gebhardt et al., 2011). In contrast to interstitial migration, T cell entry into afferent LVs and tissue exit has thus far not been investigated by IVM. In this study, we describe a mouse model that allows for simultaneous visualization of endogenous T cells and LVs by IVM. Using this model, we observed that T cells migrate in a semi-directed manner within afferent lymphatic capillaries and are carried away by flow once they have reached downstream collecting vessels. Moreover, we demonstrate that during inflammation, intralymphatic T cell crawling and migration to dLNs depend on ICAM-1 and LFA-1.

RESULTS

Characterization of the Mouse Model

To visualize T cell migration within LVs, we crossed Prox1-GFP mice, which express GFP under the control of the lymphatic-specific Prox1 promoter (Choi et al., 2011), with mice expressing a red fluorescent protein (DsRed) in all T cells, under the control of a human CD2 promoter (Veiga-Fernandes et al., 2007). The

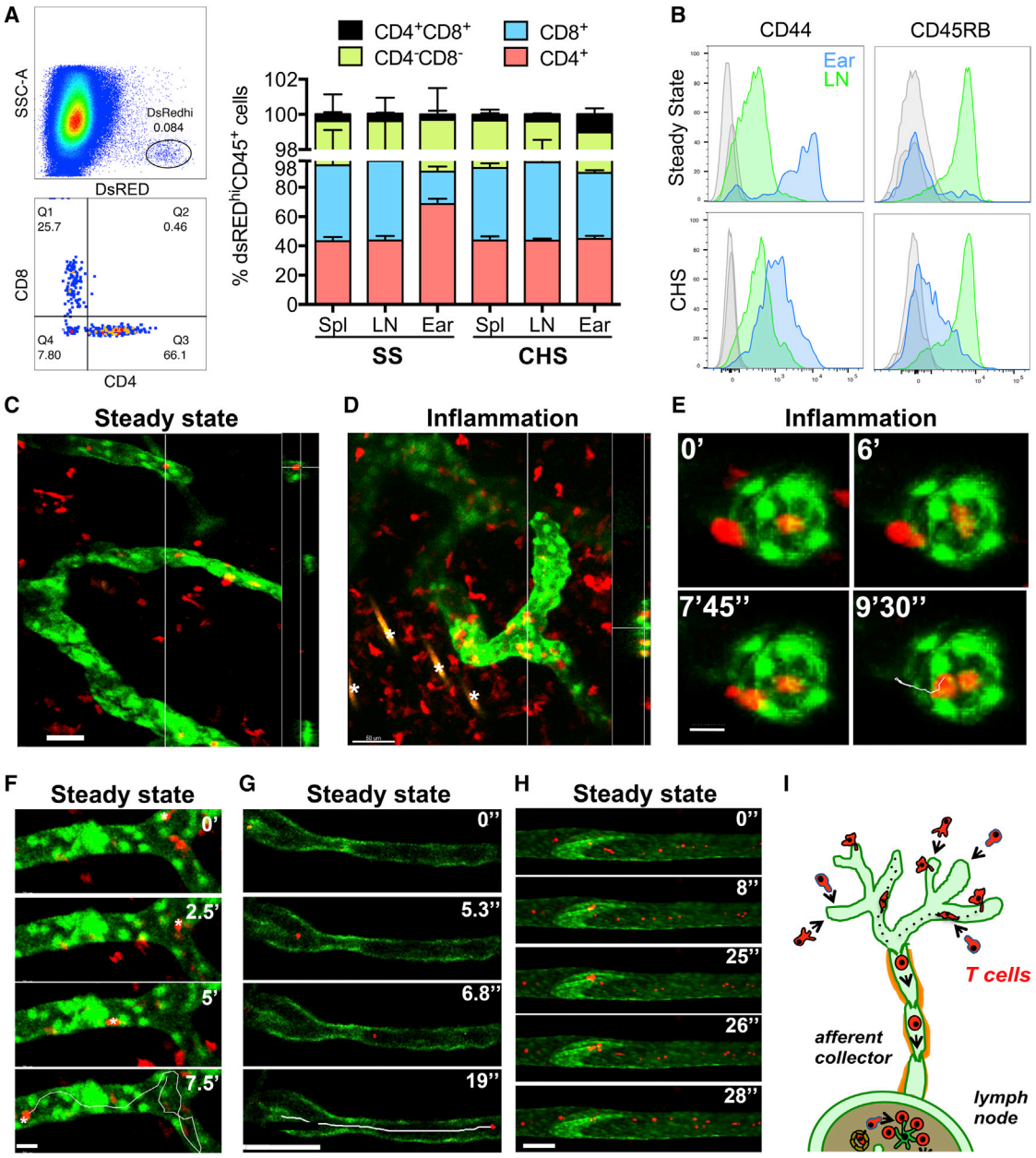

Figure 1. Characterization of hCD2-DsRedxProx1-GFP Mouse Model

(A and B) FACS analysis was performed on single-cell suspensions of steady-state or CHS-inflamed ear skin. (A) Left: representative FACS plots of steady-state ear skin showing CD4 and CD8 expression in the DsRed^{hi} population. Right: analysis of the percentage of CD4^{+}, CD8^{+}, CD4^{+}CD8^{+}, and CD4^{-}CD8^{-} among all live, DsRed^{hi}CD45^{+} cells in spleen (Spl), LNs (popliteal, inguinal, and brachial pooled) or ear skin under steady-state or CHS-inflamed conditions. Mean ± SEM is shown. (B) Most dermal CD4^{+}DsRed^{hi} T cells express a memory phenotype. Data from three to seven similar experiments are shown.

(C and D) Representative images taken from IVM performed in (C) steady-state or (D) CHS-inflamed ear skin (scale bar, 50 μm).

(E–H) Time-lapse images showing T cell (E) intravasation (scale bar, 15 μm), (F) intralymphatic crawling (same cell marked with an asterisk; scale bar, 20 μm), and free flow in afferent (G) or efferent collectors (H) (scale bar, 100 μm).

(I) Model of T cell migration through afferent LVs.

resulting hCD2-DsRedxProx1-GFP mice feature red T cells and green lymphatics (Figure S1A). Flow cytometry revealed that CD4^{+} and CD8^{+} T cells accounted for ~90% of all DsRed^{hi} cells in the ear skin, lymph nodes (LNs), and spleen of these mice (Figures 1A and S1B). While in LNs and spleen most DsRed^{hi}CD4^{+} T cells were naive (CD44^{low}CD45RB^{high}), they mainly displayed an effector-memory phenotype in the skin (CD44^{hi}CD45RB^{lo}; Figure 1B). In intravital confocal imaging performed in murine ear skin, both GFP^{+} LVs and DsRed^{hi} T cells were brightly fluorescent (Figure 1C). To image under inflammatory conditions, we

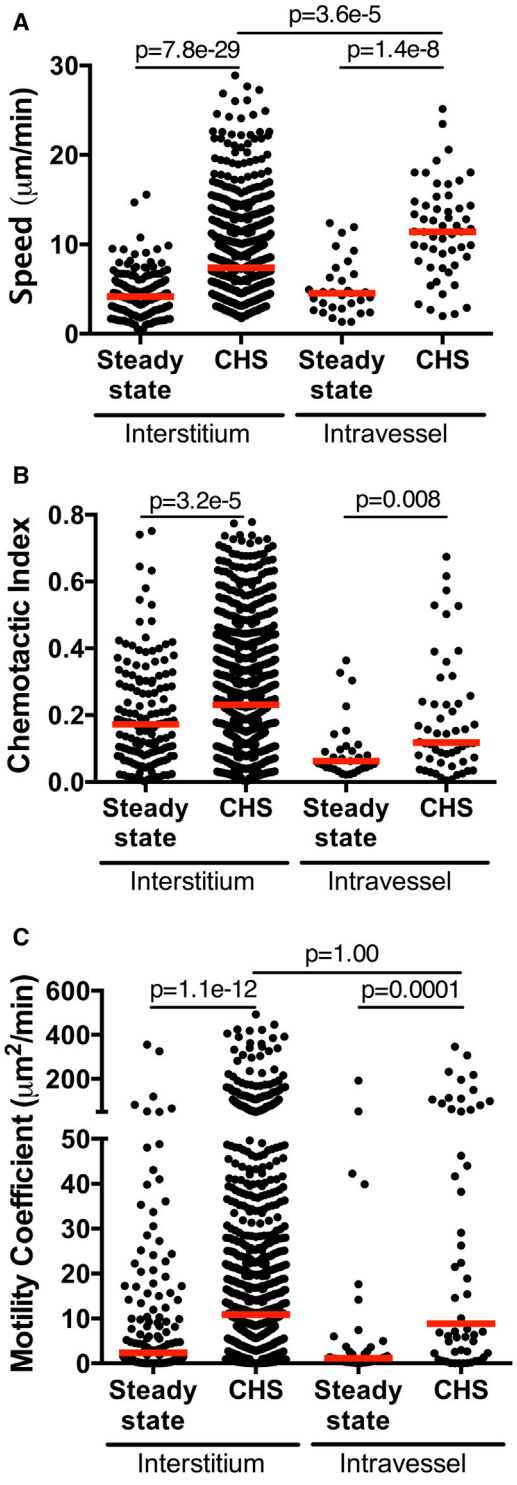

Figure 2. Inflammation Enhances T Cell Motility in the Interstitium and within Lymphatic Capillaries

IVM was performed in the ear skin under steady-state or CHS-inflamed conditions and the speed (A), chemotactic index (B), and motility coefficient (C) of T cells in the interstitium and within LVs were analyzed. Each dot represents a tracked cell. Pooled data from four mice per condition are shown.

elicited a contact hypersensitivity (CHS) response toward oxazolone. This led to a striking increase in the number of intra- and extravascular DsRed^{hi} T cells (Figure 1D). Also in inflamed skin, DsRed^{hi} cells were mainly CD8^{+} and CD4^{+} T cells displaying an effector-memory phenotype (Figures 1A and 1B). Inflammation also induced the recruitment of a population of DsRed^{lo} cells into the skin (Figure S1C). DsRed^{lo} cells displayed a larger side scatter (SSC-A) and were negative for CD3, CD11c, and Ly6G but positive for CD11b and NK1.1 (Figure S1C), suggesting that these were natural killer (NK) cells. To investigate the localization and movement of DsRed^{hi} and CD11b^{+}DsRed^{lo} cells in inflamed ear skin, we performed time-lapse imaging upon injection of an Alexa-Fluor-647-labeled anti-CD11b antibody. This revealed that CD11b^{+}DsRed^{lo} cells preferentially localized around hair follicles (Figure S1D). Only a few CD11b^{+}DsRed^{lo} cells were moving in the interstitium, with a markedly reduced motility compared to DsRed^{hi} cells (Movie S1; Figure S1E). Moreover, 36 hr after onset of inflammation, virtually no DsRed^{lo}CD11b^{+} cells had migrated to dLNs in fluorescein isothiocyanate (FITC) painting experiments (Figures S1F and S1G). In fact, all cells detected within LVs were DsRed^{hi}, whereas no intralymphatic CD11b^{+}DsRed^{lo} cells were observed (Movies S2 and S3; data not shown). Therefore, only DsRed^{hi} cells were considered T cells and included in our further analyses.

T Cells Crawl within Lymphatic Capillaries and Flow within Lymphatic Collectors

We next imaged intravasation of DsRed^{hi} T cells into LVs in CHS-inflamed ear skin (Figure 1E; Movie S4). T cell intravasation preferentially occurred in areas close to the blind ends of lymphatic capillaries, as described for DCs (Pflicke and Sixt, 2009). Once within dermal lymphatic capillaries, T cells moved by active crawling, as previously described for intralymphatic DCs (Nitschké et al., 2012; Russo et al., 2016; Tal et al., 2011) (Figure 1F; Movies S2 and S3). To visualize the behavior of T cells within lymphatic collectors, we imaged near the base of the ear pinnae, where mostly collector vessels are present. Here, we observed T cells crawling in lymphatic segments and subsequently getting detached and passively drawn into the collector upon collector pumping (Figure 1G; Movie S5). Using faster acquisition settings, we observed T cells flowing within pumping afferent LVs in the ear (Movie S6). To further visualize T cells in efferent LVs, we imaged the efferent LV leaving the inguinal LN by stereomicroscopy. In this large collector, the passive movement of T cells was synchronized with the pumping of the collector, and the valves largely impeded back flow of T cells (Figure 1H; Movie S7). The average T cell speed was ~180 μm/s, but peak velocities of up to 1 mm/s were reached in the valve regions. Overall, these experiments revealed that T cell migration to dLNs involves entry at the level of the lymphatic capillaries, active crawling and patrolling within capillaries, and passive flow once the cells reach contracting collecting vessels (Figure 1I).

Inflammation Increases T Cell Motility within LVs

In agreement with previous IVM studies (Overstreet et al., 2013), interstitial T cell motility in steady state was rather low (Figures 2A–2C; Movie S2). T cells in the initial lymphatic capillaries also displayed low motility (Figures 2A–2C; Movie S2). Interestingly,

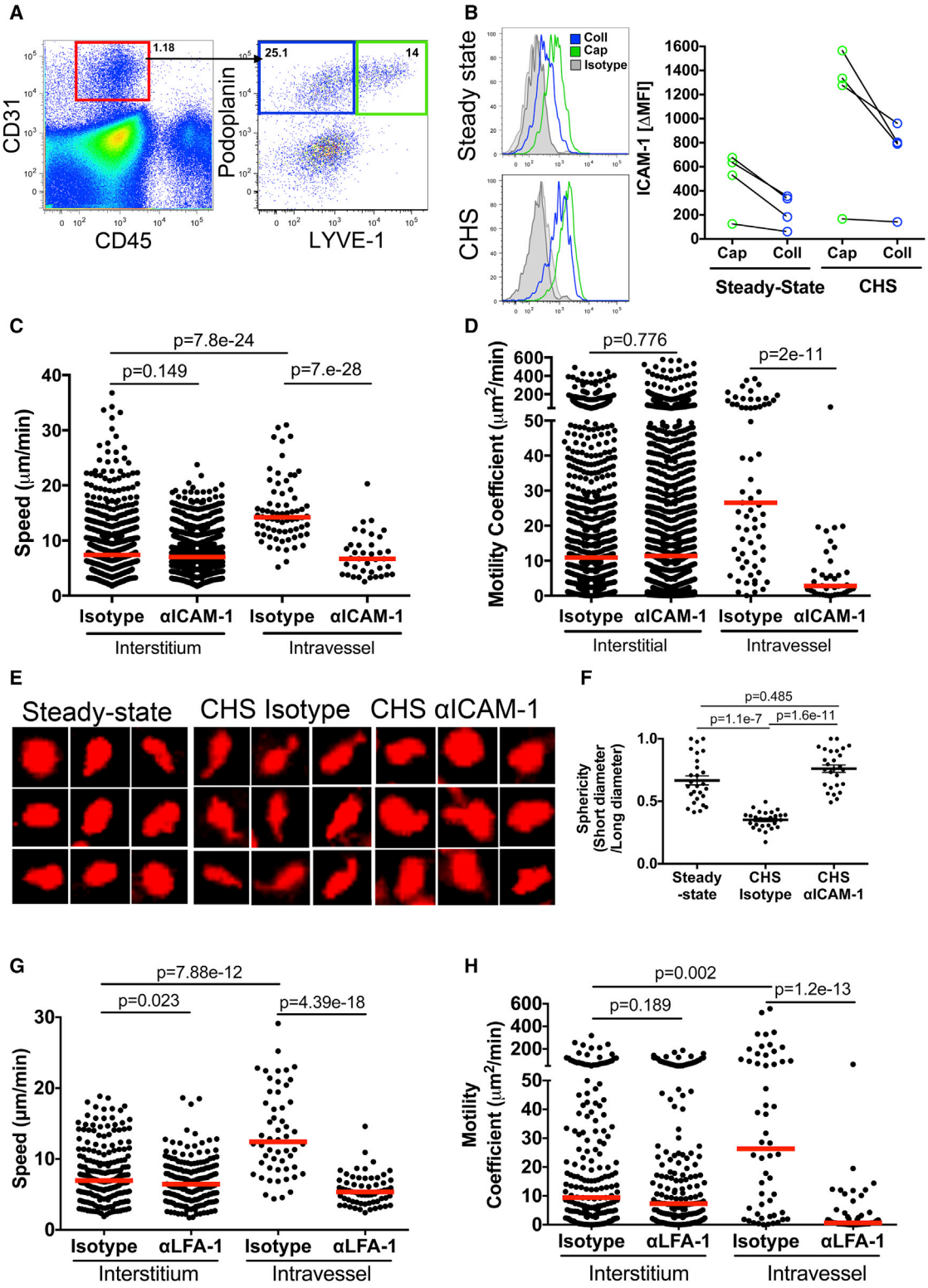

Figure 3. Increased Motility of T Cells within LVs Is ICAM-1 Dependent

(A and B) FACS analysis was performed on mouse ear skin single-cell suspensions. ICAM-1 expression was analyzed in LECs derived from lymphatic capillaries ($CD45^{-}CD31^{+}$podoplanin^{+}LYVE-1^{+}; green) or from lymphatic collectors ($CD45^{-}CD31^{+}$podoplanin^{+}LYVE-1^{-}; blue). (A) Gating scheme. (B) Left: representative FACS plots of ICAM-1 expression in LECs derived from capillaries (Cap; green) and collectors (Coll; blue); Corresponding isotypes are shown (isotype; gray).

(legend continued on next page)

in CHS-induced tissue inflammation, the motility of DsRed^{hi} T cells increased in the interstitium and even more so within lymphatic capillaries (Figures 2A–2C; Movie S3). Increases in T cell motility appeared to be a consequence of tissue inflammation, since it was also observed in inflammation induced by injection of complete Freund's adjuvant (CFA) (Figures S2A–S2C).

T Cell Motility within Lymphatic Vessels of Inflamed Skin Is ICAM-1 and LFA-1 Dependent

We and others have previously shown that ICAM-1 is upregulated in LVs during CHS- and CFA-induced skin inflammation (Johnson et al., 2006; Vigl et al., 2011). This prompted us to investigate whether ICAM-1 was involved in the increase in intralymphatic T cell motility observed in the context of inflammation. Interestingly, we found that ICAM-1 levels were consistently higher in lymphatic endothelial cells (LECs) derived from lymphatic capillaries than in LECs derived from collecting vessels and thus in the vessel segment in which T cells and DCs move by active crawling (Figures 3A and 3B). Since ICAM-1 mediates T cell crawling on blood vascular endothelium (Shulman et al., 2009; Steiner et al., 2010), we next investigated whether ICAM-1 blockade would affect T cell crawling within inflamed lymphatic capillaries. While no change in the motility of interstitial T cells was observed upon ICAM-1 blockade, the speed and motility coefficient of intralymphatic T cells were reduced to values previously measured in uninflamed, steady-state conditions (Figures 3C, 3D, and 2A, and 2B). We also noticed that T cells migrating within LVs in CHS-inflamed ears displayed the characteristic shape of a cell migrating in an integrin dependent fashion, i.e., an evident uropod and a leading edge (Figure 3E). In contrast, intralymphatic T cells in non-inflamed ears or upon ICAM-1 blockade, displayed a more rounded shape (Figures 3E and 3F). Further IVM experiments revealed that blockade of LFA-1 (i.e., the T cell-expressed ligand of ICAM-1) resulted in a comparable reduction of intralymphatic T cell crawling, suggesting the requirement of ICAM-1/LFA-1 interactions in this process (Figures 3G and 3H).

To investigate whether ICAM-1 blockade would impact the overall ability of T cells to advance through the lymphatic network, we performed experiments with in vitro Th1-polarized DsRed^{+} effector T cells (Gómez et al., 2015) (Figures S3A–S3C) in ear skin explants of Prox1-GFP mice. In our setup, Th1 cells were added on the peripheral ear skin region of the explant and left to enter into the underlying lymphatic capillaries in presence of anti-ICAM-1 or control immunoglobulin G (IgG). When analyzing the more centrally located collecting vessels 24 hr later, we consistently detected fewer T cells within collectors of anti-ICAM-1-treated as compared to control-treated explants, suggesting that ICAM-1 blockade had interfered with T cell advancement from their point of entry at the level of the lymphatic capillaries into the collectors (Figures S3D–S3H).

ICAM-1 Blockade Impairs T Cell Crawling, Adhesion, and Transmigration In Vitro

To further validate our findings, we established an in vitro assay system involving Th1 cells and conditionally immortalized murine LECs (imLECs) (Vigl et al., 2011) (Figures S3A–S3C and S4A). Also in vitro, Th1 cell motility on lymphatic endothelium was significantly reduced upon ICAM-1 blockade (Figures 4A and 4B). Surprisingly, T cells crawled equally fast on resting and on tumor necrosis factor alpha/interferon gamma (TNF-α/IFN-γ)-treated imLEC monolayers, likely because imLECs, in contrast to LECs in the skin, already express high levels of ICAM-1 under resting conditions (Figure S4A). Although TNF-α/IFN-γ treatment induced a strong upregulation of VCAM-1 in imLECs (Figure S4A), VCAM-1 blockade did not further reduce the speed of T cell crawling under inflammatory conditions (Figures S4B and S4C). Similarly, IVM performed in the presence of VCAM-1 blocking antibody (6C7.1) did not reveal any contribution of VCAM-1 to intralymphatic crawling (Figure S4F).

ICAM-1 reportedly mediates leukocyte extravasation from blood vessels (Shulman et al., 2009; Steiner et al., 2010) as well as DC migration through LVs (Johnson et al., 2006; Teijeira et al., 2013). We therefore next investigated whether ICAM-1 also promoted effector T cell adhesion and transmigration across lymphatic endothelium. Under control conditions, ICAM-1 blockade strongly inhibited T cell adhesion (Figure 4C). By contrast, under TNF-α/IFN-γ-treated conditions, when VCAM-1 was highly upregulated (Figure S4A), combined ICAM-1/VCAM-1 blockade was needed to profoundly inhibit T cell adhesion to LECs (Figure 4C). Conversely, in in vitro transmigration assays, ICAM-1 blockade equally inhibited Th1 transmigration across resting or TNF-α/IFN-γ-treated imLEC monolayers (Figure 4D), without any further contribution of VCAM-1 to the transmigration process (Figures S4D and S4E).

ICAM-1 or LFA-1 Blockade Reduces T Cell Migration from Inflamed Skin to dLNs

Finally, we assessed the overall relevance of ICAM-1 in in vivo T cell migration through afferent LVs to dLNs. For this, we co-injected activated T cells and ICAM-1 blocking or control antibody into CHS-inflamed ear skin and quantified T cell numbers in the dLN 18 hr later. In this setup ICAM-1 blockade significantly reduced T cell migration to the dLN (Figures 4E and 4F). Similarly,

Right: summary of the delta median fluorescent intensities (ΔMFIs; difference in the median fluorescent intensity between the specific and the isotope control staining), measured in four independent experiments.

(C and D) IVM was performed in CHS-inflamed ear skin upon treatment with anti-ICAM-1 or isotype control antibody. Analysis of the speed (C) and motility coefficient (D) of interstitial and intralymphatic DsRed^{hi} T cells. Each dot represents a tracked cell. Pooled data from three mice per condition are shown.

(E) Representative images of cells shapes of T cells migrating within LVs in steady-state ear skin or in CHS-inflamed ear skin treated with ICAM-1-blocking or isotype control antibody.

(F) Quantification of the cell diameter ratio (length/width). Pooled data from three experiments are shown. Mean ± SEM is shown.

(G and H) Further IVM was performed in CHS-inflamed ear skin upon treatment with anti-LFA-1 or isotype control antibody. Analysis of the speed (G) and motility coefficient (H) of interstitial and intralymphatic DsRed^{hi} T cells. Each dot represents a tracked cell. Pooled data from three mice per condition are shown.

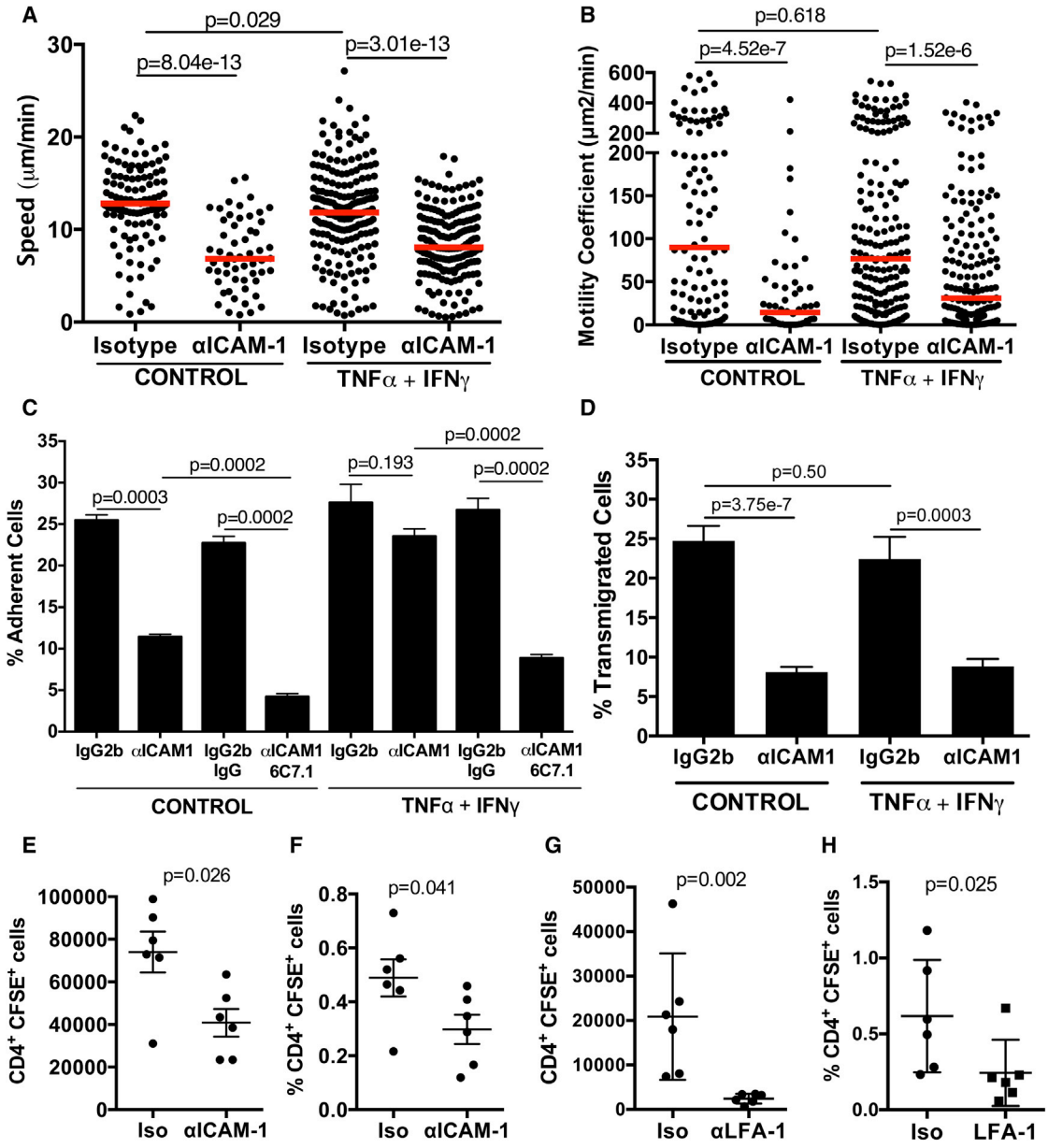

Figure 4. ICAM-1 Mediates In Vitro Interactions between T Cells and Lymphatic Endothelium, as Well as In Vivo Migration of T Cells to dLNs

(A–D) DsRed$^+$ Th1 cells were placed onto control-treated or IFNγ/TNFα-treated imLEC monolayers and the impact of anti-ICAM-1 or isotype IgG on T cell crawling, adhesion, and transmigration was analyzed. Blockade of ICAM-1 reduced the speed (A), and motility coefficient (B) of T cell crawling on lymphatic endothelium. Each dot represents a tracked cell. Data from one out of three similar experiments is shown. (C) Blockade of ICAM-1 or of ICAM-1 and VCAM-1 (referred as 6C7.1) reduced the T cell adhesion to imLEC monolayers. Data from one out of four similar experiments are shown. (D) ICAM-1 blockade reduced T cell transmigration across imLEC monolayers. Pooled data from three similar experiments are shown. Mean ± SEM is shown.

(E–H) Activated T cells were injected into CHS-inflamed ear skin in the presence of ICAM-1-blocking (E and F) or LFA-1-blocking (G and H) antibody or the respective control antibody. 18 hr later, T cell numbers were quantified in auricular dLNs by FACS. Absolute number (E and G) and percentage (F and H) of transferred T cells among total LN cells. Each dot represents an individual mouse. Data from one representative experiment out of two or three similar experiments are shown. Mean ± SEM is shown.

blockade of LFA-1 significantly reduced the number of adoptively transferred T cells that migrated to the dLN (Figures 4G and 4H). Overall, these findings demonstrate a key role for ICAM-1/LFA-1 interactions in T cell migration through afferent LVs.

DISCUSSION

In this study, we imaged T cell migration into and within dermal LVs. In contrast to T cell extravasation from blood vessels or migration within the skin, this process is far less well understood,

at both the molecular and cellular levels. Our results show that T cell migration through afferent LVs occurs in a stepwise fashion; T cells that have entered into afferent capillaries first crawl in a semi-directed manner toward lymphatic collectors, from where they are passively transported within the lymph fluid to the dLN. This multistep process recapitulates the multistep migration pattern that we and others recently described for DC migration through afferent lymphatics (Nitschké et al., 2012; Russo et al., 2016; Tal et al., 2011). The reason why DCs and T cells need to actively crawl within afferent capillaries probably lies in the weak lymph flow conditions within these vessels segments. Most likely, only the pumping lymphatic collectors generate sufficient flow and shear to support passive transport of leukocytes at high speed within lymph fluid. However, given that anesthesia is expected to slow down lymph flow, T cell speeds measured in collectors of anesthetized animals may be an underestimation of T cell speeds in collectors of awake animals. In agreement with our previous findings on DC migration (Russo et al., 2016), T cells do not migrate unidirectionally through capillaries but display an intralymphatic patrolling behavior. Whether this intralymphatic movement is indeed semi-directed, and as in the case of DCs, dependent on an intralymphatic CCL21 gradient (Russo et al., 2016) remains to be investigated.

Under steady-state conditions, we typically observed only few T cells in the interstitium or within afferent capillaries and collectors. Given that most dermal T cells display an effector-memory phenotype, this low cell number most likely represents an artifact of the hygienic mouse housing conditions of laboratory mice, in which abnormally few effector-memory cells populate peripheral tissues (Beura et al., 2016). It is therefore very likely that under less hygienic, more natural conditions, many more T cells are present within afferent lymphatics in steady state. By contrast, under inflammatory conditions, high numbers of T cells are recruited into the skin and into afferent LVs. This is consistent with afferent lymph cannulation studies in sheep reporting a dramatic increase in T cell entering the afferent lymph during inflammation (Brown et al., 2010). Our data show that the striking increase in intralymphatic crawling velocity observed in vivo in the context of inflammation was mainly due to ICAM-1 upregulation in LECs; blockade of ICAM-1 or its T cell-expressed ligand, LFA-1, reduced crawling velocities to values observed under steady-state conditions, during which LECs express low levels of ICAM-1. Besides mediating intralymphatic crawling, ICAM-1 also supported T cell adhesion and transmigration across LEC monolayers and, most importantly, the overall process of T cell migration to dLNs. Notably, we observed the contribution of ICAM-1 to T cell migration to dLNs under inflammatory conditions, but not under steady-state conditions (data not shown), likely because of the low ICAM-1 levels expressed on LVs in the absence of inflammation. Our observations are in agreement with previous findings on DCs, which migrate integrin independently into lymphatics and to dLNs in steady state (Lämmermann et al., 2008), whereas in inflammation, integrins and their LEC-expressed ligands start to play a key role in migration (Johnson et al., 2006; Johnson and Jackson, 2010; Teijeira et al., 2013). In agreement with our in vitro findings, we did not observe any effect of VCAM-1 blockade on in vivo T cell crawling within capillaries (Figures S4F and S4G). However, blockade of VCAM-1 strongly reduced the overall ability of T cells to migrate from inflamed skin to the dLN (Figures S4G and S4H). Although not experimentally addressed in this study, these findings point toward an involvement of VCAM-1 in T cell entry into LVs in vivo. In support of such an involvement, we observed that combined blockade of VCAM-1 and ICAM-1 further reduced in vitro Th1 cell adhesion to lymphatic endothelium when compared to ICAM-1 blockade alone (Figure 4C). However this experiment did not address the contribution of VCAM-1 alone to in vitro adhesion. The reason why VCAM-1 blockade did not result in a defect in in vitro transmigration (Figures S4D and S4E) could be linked with the fact that in-vitro-generated Th1 cells expressed rather low levels of the α4 integrin subunit CD49d, which forms part of the VCAM-1-binding VLA-4 integrin (Figure S3C). Additionally, in-vitro-cultured imLECs express very high ICAM-1 levels (Figure S4A), which might have overridden any potential contribution of VCAM-1 in the transmigration process.

Overall, our data reveal that LFA-1/ICAM-1 interactions are not only important for directing T cells out of blood vessels into peripheral tissues but also facilitate T cell tissue egress and recirculation during inflammation. These findings somewhat differ from those recently reported for T cell egress from LNs; here, LFA-1 and ICAM-1 were shown to prevent T cell transmigration across lymphatic sinuses into efferent lymphatics, thereby contributing to a longer T cell dwell time within the LN (Reichardt et al., 2013). The reason for these differences between the roles of LFA-1/ICAM-1 in T cell migration into afferent versus efferent lymphatics is not clear, but it could be related to the different functions and localization of the tissue egress and retention signals S1P and CCL21 in LNs and skin. In inflammatory and malignant conditions, tissue egress of T cells most likely takes place almost exclusively via afferent LVs. Given that the molecular players in LV entry and crawling are very similar to those involved in tissue entry from blood vessels, these mechanisms are very difficult to dissect from a therapeutic point of view. It is likely that approved drugs such as fingolimod (a functional antagonist of S1P receptors) or natalizumab (a monoclonal antibody blocking α4 integrin subunits) not only affect entry but also exit of T cells from inflamed tissues. Thus far, only two lymphatic endothelial cell-expressed adhesion molecules mediating T cell migration through afferent LVs have been identified, namely CLEVER-1 (Karikoski et al., 2009) and the macrophage mannose receptor (Salmi et al., 2013). Overall, our study contributes to understanding the molecular control of T cell migration into afferent lymphatics and adds insight on how this process occurs at the cellular level.

EXPERIMENTAL PROCEDURES

Mouse Strains

Wild-type (WT) C57BL/6 mice were purchased from Janvier. Prox1-GFP mice (Choi et al., 2011) and hCD2-DsRed mice (Veiga-Fernandes et al., 2007) were bred in our facility. All experiments were approved by the Cantonal Veterinary Office Zurich.

Flow Cytometry

Flow cytometry was performed on ear skin, LNs, spleen, or in-vitro-generated Th1 cells from CD2-DsRed or WT mice. Ear skin was digested with collagenase IV (Invitrogen) as previously described (Vigl et al., 2011). Single-cell

suspensions were stained as specified in Supplemental Experimental Procedures. Fluorescence-activated cell sorting (FACS) analysis was performed on a BD FACSCanto (BD Biosciences) using FACSDiva software. Data were analyzed offline using FlowJo software 10.0.1 (Tree Star).

IVM Specifications and Treatment Conditions

IVM on the dorsal side of the mouse ear pinna of anesthetized hCD2-DsRedxProx1-GFP mice was performed as previously described (Nitschké et al., 2012; Russo et al., 2016). The exact IVM specifications, treatment conditions, and specifications for T cell motility analysis are provided in Supplemental Experimental Procedures.

CHS-Induced Ear Skin Inflammation

A CHS response toward oxazolone was induced as described previously (Vigl et al., 2011). Briefly, mice were anesthetized and sensitized by topical application of 2% oxazolone (4-ethoxymethylene-2-phenyl-2-oxazoline-5-one; Sigma) in acetone/olive oil (4:1 vol/vol) on the shaved abdomen (50 μL) and on each paw (5 μL). 5 days later, 10 μL of a 1% oxazolone solution was applied topically to each side of the ears (challenge phase). Experiments were performed 24 hr after challenge.

Adoptive Transfer Experiment

$CD4^+$ cells were purified from the spleens of OTII mice using CD4 (L3T4) microbeads (Miltenyi Biotec). $CD4^+$ T cells were activated for 48 hr with 100 ng/mL $OVA_{323–339}$ peptide. After an additional 24 hr without peptide, cells were labeled with CFSE (Sigma) according to the manufacturer's instructions. 10^6 cells, together with 5 μg anti-mouse ICAM-1 antibody (clone YN1/1.7.4; BioLegend), anti-mouse LFA-1 antibody (clone M17/4; BioXCell), anti-mouse VCAM-1 (6C7.1; Engelhardt et al., 1998), or corresponding isotypes (from BioLegend or BioXCell), in 10 μL were co-injected into the dorsal half of CHS-inflamed ears of WT mice. 18 hr later, auricular LNs were harvested, stained with CD4-APC (BioLegend), and analyzed on a FACSCalibur (BD Biosciences). Counting beads were added to determine absolute cell numbers.

Generation of Th1 Cells

$CD4^+$ cells were isolated from LNs and spleen of hCD2-DsRed mice and differentiated into Th1 cells in vitro as described previously (Gómez et al., 2015) and in Supplemental Experimental Procedures.

In Vitro Experiments with Murine LECs and Th1 Cells

For details, see Supplemental Experimental Procedures.

Statistical Analysis

All cell-tracking data are presented as medians, and all other results are presented as mean plus SEM. Datasets were analyzed with Prism 6 (GraphPad). Kruskal-Wallis test followed by post hoc analysis was used for multiple comparisons and Mann-Whitney *U* test for simple comparisons.

SUPPLEMENTAL INFORMATION

Supplemental Information includes Supplemental Experimental Procedures, four figures, and seven movies and can be found with this article online at http://dx.doi.org/10.1016/j.celrep.2016.12.078.

AUTHOR CONTRIBUTIONS

A.T. and M.C.H. designed research, performed research, analyzed data, and wrote the paper. E.R., T.F., and S.T.P. performed research and analyzed and discussed data. M.C., A.R., M.D., G.F.D., and I.M. provided essential reagents and experimental guidance and/or discussed data. C.H. designed research, analyzed data, and wrote the paper.

ACKNOWLEDGMENTS

The authors thank Simone Haener and the Scientific Center for Optical and Electron Microscopy (ScopeM) for excellent technical assistance, the staff of the ETH Rodent Center HCI for animal husbandry, and Dietmar Vestweber (Max Planck Institute Münster, Germany) and Lothar Dieterich (ETH Zurich) for providing anti-VCAM-1 antibody. A.T. was supported by a fellowship from the Swiss Government Excellence Scholarship Program. C.H. gratefully acknowledges financial support from the Swiss National Science Foundation (grant 310030_156269).

Received: July 20, 2016
Revised: December 2, 2016
Accepted: December 22, 2016
Published: January 24, 2017

REFERENCES

Beura, L.K., Hamilton, S.E., Bi, K., Schenkel, J.M., Odumade, O.A., Casey, K.A., Thompson, E.A., Fraser, K.A., Rosato, P.C., Filali-Mouhim, A., et al. (2016). Normalizing the environment recapitulates adult human immune traits in laboratory mice. Nature *532*, 512–516.

Bromley, S.K., Yan, S., Tomura, M., Kanagawa, O., and Luster, A.D. (2013). Recirculating memory T cells are a unique subset of CD4+ T cells with a distinct phenotype and migratory pattern. J. Immunol. *190*, 970–976.

Brown, M.N., Fintushel, S.R., Lee, M.H., Jennrich, S., Geherin, S.A., Hay, J.B., Butcher, E.C., and Debes, G.F. (2010). Chemoattractant receptors and lymphocyte egress from extralymphoid tissue: changing requirements during the course of inflammation. J. Immunol. *185*, 4873–4882.

Choi, I., Chung, H.K., Ramu, S., Lee, H.N., Kim, K.E., Lee, S., Yoo, J., Choi, D., Lee, Y.S., Aguilar, B., and Hong, Y.K. (2011). Visualization of lymphatic vessels by Prox1-promoter directed GFP reporter in a bacterial artificial chromosome-based transgenic mouse. Blood *117*, 362–365.

Debes, G.F., Arnold, C.N., Young, A.J., Krautwald, S., Lipp, M., Hay, J.B., and Butcher, E.C. (2005). Chemokine receptor CCR7 required for T lymphocyte exit from peripheral tissues. Nat. Immunol. *6*, 889–894.

Egawa, G., Honda, T., Tanizaki, H., Doi, H., Miyachi, Y., and Kabashima, K. (2011). In vivo imaging of T-cell motility in the elicitation phase of contact hypersensitivity using two-photon microscopy. J. Invest. Dermatol. *131*, 977–979.

Engelhardt, B., Laschinger, M., Schulz, M., Samulowitz, U., Vestweber, D., and Hoch, G. (1998). The development of experimental autoimmune encephalomyelitis in the mouse requires alpha4-integrin but not alpha4beta7-integrin. J. Clin. Invest. *102*, 2096–2105.

Gebhardt, T., Whitney, P.G., Zaid, A., Mackay, L.K., Brooks, A.G., Heath, W.R., Carbone, F.R., and Mueller, S.N. (2011). Different patterns of peripheral migration by memory CD4+ and CD8+ T cells. Nature *477*, 216–219.

Gómez, D., Diehl, M.C., Crosby, E.J., Weinkopff, T., and Debes, G.F. (2015). Effector T cell egress via afferent lymph modulates local tissue inflammation. J. Immunol. *195*, 3531–3536.

Johnson, L.A., and Jackson, D.G. (2010). Inflammation-induced secretion of CCL21 in lymphatic endothelium is a key regulator of integrin-mediated dendritic cell transmigration. Int. Immunol. *22*, 839–849.

Johnson, L.A., Clasper, S., Holt, A.P., Lalor, P.F., Baban, D., and Jackson, D.G. (2006). An inflammation-induced mechanism for leukocyte transmigration across lymphatic vessel endothelium. J. Exp. Med. *203*, 2763–2777.

Karikoski, M., Irjala, H., Maksimow, M., Miiluniemi, M., Granfors, K., Hernesniemi, S., Elima, K., Moldenhauer, G., Schledzewski, K., Kzhyshkowska, J., et al. (2009). Clever-1/Stabilin-1 regulates lymphocyte migration within lymphatics and leukocyte entrance to sites of inflammation. Eur. J. Immunol. *39*, 3477–3487.

Lämmermann, T., Bader, B.L., Monkley, S.J., Worbs, T., Wedlich-Söldner, R., Hirsch, K., Keller, M., Förster, R., Critchley, D.R., Fässler, R., and Sixt, M. (2008). Rapid leukocyte migration by integrin-independent flowing and squeezing. Nature *453*, 51–55.

Ledgerwood, L.G., Lal, G., Zhang, N., Garin, A., Esses, S.J., Ginhoux, F., Merad, M., Peche, H., Lira, S.A., Ding, Y., et al. (2008). The sphingosine

1-phosphate receptor 1 causes tissue retention by inhibiting the entry of peripheral tissue T lymphocytes into afferent lymphatics. Nat. Immunol. *9*, 42–53.

Mackay, C.R., Marston, W.L., and Dudler, L. (1990). Naive and memory T cells show distinct pathways of lymphocyte recirculation. J. Exp. Med. *171*, 801–817.

Nitschké, M., Aebischer, D., Abadier, M., Haener, S., Lucic, M., Vigl, B., Luche, H., Fehling, H.J., Biehlmaier, O., Lyck, R., and Halin, C. (2012). Differential requirement for ROCK in dendritic cell migration within lymphatic capillaries in steady-state and inflammation. Blood *120*, 2249–2258.

Overstreet, M.G., Gaylo, A., Angermann, B.R., Hughson, A., Hyun, Y.M., Lambert, K., Acharya, M., Billroth-Maclurg, A.C., Rosenberg, A.F., Topham, D.J., et al. (2013). Inflammation-induced interstitial migration of effector $CD4^+$ T cells is dependent on integrin αV. Nat. Immunol. *14*, 949–958.

Pflicke, H., and Sixt, M. (2009). Preformed portals facilitate dendritic cell entry into afferent lymphatic vessels. J. Exp. Med. *206*, 2925–2935.

Reichardt, P., Patzak, I., Jones, K., Etemire, E., Gunzer, M., and Hogg, N. (2013). A role for LFA-1 in delaying T-lymphocyte egress from lymph nodes. EMBO J. *32*, 829–843.

Russo, E., Teijeira, A., Vaahtomeri, K., Willrodt, A.H., Bloch, J.S., Nitschké, M., Santambrogio, L., Kerjaschki, D., Sixt, M., and Halin, C. (2016). Intralymphatic CCL21 promotes tissue egress of dendritic cells through afferent lymphatic vessels. Cell Rep. *14*, 1723–1734.

Salmi, M., Karikoski, M., Elima, K., Rantakari, P., and Jalkanen, S. (2013). CD44 binds to macrophage mannose receptor on lymphatic endothelium and supports lymphocyte migration via afferent lymphatics. Circ. Res. *112*, 1577–1582.

Shulman, Z., Shinder, V., Klein, E., Grabovsky, V., Yeger, O., Geron, E., Montresor, A., Bolomini-Vittori, M., Feigelson, S.W., Kirchhausen, T., et al. (2009). Lymphocyte crawling and transendothelial migration require chemokine triggering of high-affinity LFA-1 integrin. Immunity *30*, 384–396.

Steiner, O., Coisne, C., Cecchelli, R., Boscacci, R., Deutsch, U., Engelhardt, B., and Lyck, R. (2010). Differential roles for endothelial ICAM-1, ICAM-2, and VCAM-1 in shear-resistant T cell arrest, polarization, and directed crawling on blood-brain barrier endothelium. J. Immunol. *185*, 4846–4855.

Tal, O., Lim, H.Y., Gurevich, I., Milo, I., Shipony, Z., Ng, L.G., Angeli, V., and Shakhar, G. (2011). DC mobilization from the skin requires docking to immobilized CCL21 on lymphatic endothelium and intralymphatic crawling. J. Exp. Med. *208*, 2141–2153.

Teijeira, A., Garasa, S., Peláez, R., Azpilikueta, A., Ochoa, C., Marré, D., Rodrigues, M., Alfaro, C., Aubá, C., Valitutti, S., et al. (2013). Lymphatic endothelium forms integrin-engaging 3D structures during DC transit across inflamed lymphatic vessels. J. Invest. Dermatol. *133*, 2276–2285.

Veiga-Fernandes, H., Coles, M.C., Foster, K.E., Patel, A., Williams, A., Natarajan, D., Barlow, A., Pachnis, V., and Kioussis, D. (2007). Tyrosine kinase receptor RET is a key regulator of Peyer's patch organogenesis. Nature *446*, 547–551.

Vigl, B., Aebischer, D., Nitschké, M., Iolyeva, M., Röthlin, T., Antsiferova, O., and Halin, C. (2011). Tissue inflammation modulates gene expression of lymphatic endothelial cells and dendritic cell migration in a stimulus-dependent manner. Blood *118*, 205–215.

Yawalkar, N., Hunger, R.E., Pichler, W.J., Braathen, L.R., and Brand, C.U. (2000). Human afferent lymph from normal skin contains an increased number of mainly memory / effector CD4(+) T cells expressing activation, adhesion and co-stimulatory molecules. Eur. J. Immunol. *30*, 491–497.

Young, A.J. (1999). The physiology of lymphocyte migration through the single lymph node in vivo. Semin. Immunol. *11*, 73–83.